



Published in final edited form as:

J Refract Surg. 2010 August ; 26(8): 555–564. doi:10.3928/1081597X-20091105-02.

Epithelial Thickness After Hyperopic LASIK: Three-dimensional Display With Artemis Very High-frequency Digital Ultrasound

Dan Z. Reinstein, MD, MA(Cantab), FRCSC, FRCOphth, Timothy J. Archer, MA(Oxon), DipCompSci(Cantab), Marine Gobbe, MST(Optom), PhD, Ronald H. Silverman, PhD, and D. Jackson Coleman, MD

London Vision Clinic, London (Reinstein, Archer, Gobbe); the Department of Ophthalmology, St Thomas' Hospital - Kings College, London (Reinstein), United Kingdom; the Department of Ophthalmology, Weill Medical College of Cornell University, New York, New York (Reinstein, Silverman, Coleman); Centre Hospitalier National d'Ophthalmologie, Paris, France (Reinstein); and Riverside Research Institute, New York, New York (Silverman)

Abstract

PURPOSE—To characterize the epithelial thickness profile in a population of eyes after LASIK for hyperopia or hyperopic astigmatism.

METHODS—The epithelial thickness profile was measured in vivo by Artemis very high-frequency (VHF) digital ultrasound scanning (ArcScan Inc) across the central 10-mm diameter of the cornea on 65 eyes at least 3 months after hyperopic LASIK using a 7-mm ablation zone with the MEL 80 excimer laser (Carl Zeiss Meditec). Maps of the average, standard deviation, minimum, maximum, and range of epithelial thickness were plotted. The cross-sectional hemi-meridional epithelial thickness profile was calculated using annular averaging. Linear regression analysis was performed to evaluate correlations between epithelial thickness, spherical equivalent refraction treated, and maximum simulated keratometry.

RESULTS—The mean thinnest epithelial thickness was $39.7 \pm 5.6 \mu\text{m}$ and the mean thickest epithelial thickness was $89.3 \pm 14.6 \mu\text{m}$. The average epithelial thickness profile showed an epithelial doughnut pattern characterized by localized central thinning within the 4-mm diameter zone surrounded by an annulus of thick epithelium, with the thickest epithelium at the 3.4-mm radius. The epithelium was on average 10- μm thicker temporally than nasally at the 3.4-mm radius. Central epithelium was thinner and paracentral epithelium was thicker for higher hyperopic corrections and steeper maximum simulated keratometry.

Correspondence: Dan Z. Reinstein, MD, MA(Cantab), FRCSC, FRCOphth, London Vision Clinic, 138 Harley St, London W1G 7LA, United Kingdom. Tel: 44 207 224 1005; Fax: 44 207 224 1055; dzt@londonvisionclinic.com.

Drs Reinstein, Silverman, and Coleman have a proprietary interest in the Artemis technology (ArcScan Inc, Morrison, Colorado) and are the authors of patents related to very high-frequency digital ultrasound administered by the Cornell Center for Technology Enterprise and Commercialization (CCTEC), Ithaca, New York. Dr Reinstein is a consultant for Carl Zeiss Meditec (Jena, Germany). The remaining authors have no proprietary or financial interest in the materials presented herein.

Preparation in part fulfillment of the requirements for the doctoral thesis, University of Cambridge, for Dr Reinstein.

AUTHOR CONTRIBUTIONS

Study concept and design (D.Z.R., T.J.A., M.G., R.H.S., D.J.C.); data collection (T.J.A.); analysis and interpretation of data (D.Z.R., T.J.A.); drafting of the manuscript (D.Z.R., T.J.A.); critical revision of the manuscript (D.Z.R., M.G., R.H.S., D.J.C.); statistical expertise (T.J.A.)

CONCLUSIONS—Three-dimensional high-resolution ultrasound mapping of epithelial thickness profile after LASIK for hyperopia demonstrated thinner epithelium centrally and thicker epithelium paracentrally. Presumably, the paracentral epithelial thickening compensated in part for the stromal tissue removed by the hyperopic ablation, whereas the central epithelial thinning compensated for the localized increase in corneal curvature.

It is known that the corneal epithelium has the ability to alter its thickness profile to re-establish a smooth, symmetrical optical surface and either partially or totally mask the presence of an irregular stromal surface from front surface topography.¹ Numerous reports have been published describing central epithelial thickening following central tissue removal by myopic excimer laser ablations, which has been related to myopic regression.²⁻¹² Epithelial thickness changes have also been described after radial keratotomy,¹³ intracorneal ring segments,^{14,15} and orthokeratology contact lens wear.¹⁶⁻²⁰ The epithelium has also been reported to compensate for stromal irregularities in cases of asymmetric resection in automated lamellar keratoplasty,⁴ asymmetric LASIK flaps,^{4,21,22} microfolds,^{21,22} flap malposition and short flap,²¹⁻²³ free cap malrotation,²⁴ and irregular stromal surface following multiple refractive procedures.¹

In keratoconus, epithelial thinning in the region of the cone has been reported,²⁵⁻²⁷ and we have previously shown that the epithelial thickness profile across the central 8-mm diameter follows an epithelial doughnut pattern characterized by epithelial thinning over the cone surrounded by an annulus of epithelial thickening.^{28,29}

Given the reported epithelial thickness changes after myopic excimer laser ablation, it is likely that epithelial changes would also be observed after hyperopic excimer laser ablation. A hyperopic ablation is designed to steepen the central cornea, which bears a similarity to the morphology of a keratoconic cornea, so the epithelial thickness profile after hyperopic ablation might be expected to follow a similar pattern to that seen in keratoconus. Indeed, we have previously described the epithelial thickness across the horizontal meridian of an eye 3 months after hyperopic LASIK in which the epithelium was thicker paracentrally, coincident with the zone of stromal tissue removal.⁴ No reports have been found describing changes in the epithelial thickness profile across the whole cornea after hyperopic LASIK.

Artemis very high-frequency (VHF) digital ultrasound (ArcScan Inc, Morrison, Colorado) is, to date, the only published method measuring individual corneal layers, including the epithelium and stroma, continuously over a large area of cornea (8 to 10 mm).^{2,3,28-35} We have previously used the Artemis to describe the average epithelial thickness profile in a population of normal eyes³³ as well as a population of keratoconic eyes.^{28,29} The repeatability of epithelial thickness measurements in the normal population has been shown to be $<1.32 \mu\text{m}$ within the central 6-mm diameter, with a central repeatability of $0.58 \mu\text{m}$.³⁵

The purpose of this study was to qualitatively and quantitatively characterize the thickness profile of the epithelium in a population of eyes after hyperopic LASIK with the MEL 80 (Carl Zeiss Meditec, Jena, Germany) excimer laser using the Artemis VHF digital ultrasound arc-scanning system.

PATIENTS AND METHODS

This was a retrospective case series of 65 eyes of 34 consecutive patients who underwent an Artemis VHF digital ultrasound scan at least 3 months after hyperopic LASIK at the London Vision Clinic, London, United Kingdom, between June 2003 and August 2007. In all cases, LASIK was performed by an experienced surgeon (D.Z.R.) using the MEL 80 excimer laser and the Hansatome or Hansatome zero-compression microkeratome (Bausch & Lomb, Salt Lake City, Utah) with the 160- μ m head and 9.5-mm ring. An optical zone of 7 mm was used in all eyes with the maximum ablation depth at the 3.5-mm radius. At the postoperative assessment, topography and keratometry were performed using the Orbscan II (Bausch & Lomb). Three-dimensional epithelial thickness for the central 10-mm diameter was measured using the Artemis 1 VHF digital ultrasound arc-scanner. Postoperative Artemis scans were performed 1) for all patients where an Artemis scan had been obtained before LASIK; 2) to evaluate suitability for retreatment; or 3) as part of a separate study to investigate the flap thickness reproducibility of the Hansatome zero-compression microkeratome.

All patients gave informed consent for the use of their data for research, analysis, and publication purposes.

Artemis VHF Digital Ultrasound Arc-Scanning

The Artemis VHF digital ultrasound system has been previously described in detail.^{33,35} Briefly, Artemis VHF digital ultrasound is carried out using an ultrasonic standoff medium. The patient sits and positions the chin and forehead into a headrest while placing the eye in a soft rimmed eye-cup. Warm sterile normal saline (33°C) is filled into the darkened scanning chamber. The patient fixates on a narrowly focused aiming beam, which is coaxial with the infrared camera, the corneal vertex, and the center of rotation of the scanning system. The technician adjusts the center of rotation of the system until it is coaxial with the corneal vertex. In this manner, the position of each scan plane is maintained about a single point on the cornea and corneal mapping is therefore centered on the corneal vertex. The Artemis VHF digital ultrasound uses a broadband 50-MHz VHF ultrasound transducer (bandwidth approximately 10 to 60 MHz), which is swept by a reverse arc, high-precision mechanism to acquire B-scans as arcs that follow the surface contour of anterior or posterior segment structures of interest. Performing a three-dimensional scan set with the Artemis 1 takes approximately 2 to 3 minutes per each eye.

Using VHF digital ultrasound, interfaces between tissues are detected at the location of the maximum change in acoustic impedance (the product of the density and the speed of sound). It was first demonstrated in 1993 that acoustic interfaces detected in the cornea were located spatially at the epithelial surface and at the interface between epithelial cells and the anterior surface of Bowman layer.³⁰ Therefore, the measurement of the epithelium with the Artemis VHF digital ultrasound scanner includes Bowman layer.

Three-Dimensional Pachymetric Topography

For three-dimensional scan sets, the scan sequence consisted of four meridional B-scans at 45° intervals. Each scan sweep takes approximately 0.25 seconds and consists of 128 scan lines or pulse echo vectors. Ultrasound data are digitized and stored. The digitized ultrasound data are then transformed using digital signal processing technology and software developed by our group at Weill-Cornell Medical College, which includes auto-correlation of back-surface curvatures to center and align the meridional scans. A speed of sound constant of 1640 m/s was used.

Statistical Analysis

Descriptive statistics (average, minimum, maximum, standard deviation, and range) were calculated for each point in the 10×10 mm Cartesian matrix across eyes. These statistics were carried out for all eyes using vertical mirrored symmetry superimposition—thickness values for left eyes were reflected in the vertical axis and superimposed onto right eye values so that nasal/temporal characteristics could be combined. The resultant matrices were plotted using DeltaGraph v5.0 (SPSS Inc, Chicago, Illinois) as surface fill X,Y,Z plots to represent the point-by-point average, standard deviation, minimum, maximum, and range of the population. The value and location of the thinnest and thickest epithelium were determined for each eye.

The cross-sectional, hemimeridional average epithelial thickness profile was determined for each eye by averaging the epithelial thickness within the 0.03-mm zone centered on the corneal vertex and within 35 annular bands, each 0.06-mm wide, centered on the corneal vertex with central radii increasing in 0.1-mm steps. The average epithelial thickness within each annular band was plotted against the radial distance from the corneal vertex.

Linear regression analysis was performed between 1) the thinnest epithelium and the attempted spherical equivalent refraction; 2) the thickest epithelium and the attempted spherical equivalent refraction; 3) the thinnest epithelium and the postoperative maximum simulated keratometry; and 4) the thickest epithelium and the postoperative maximum simulated keratometry. The linear regression equation and coefficient of determination (R^2) was calculated for each correlation.

As this was a retrospective case series, preoperative epithelial thickness data were not available for all eyes in this population. To investigate the change in epithelial thickness due to the ablation, the preoperative, postoperative, and change in epithelial thickness were mapped for the subset of 10 eyes where preoperative data were available.

Descriptive statistics, comparative statistics, and linear regression analysis were performed in Microsoft Excel 2003 (Microsoft Corp, Redmond, Washington). A P value $<.05$ was considered statistically significant.

RESULTS

During the study period, 65 eyes of 34 patients (31 right and 34 left eyes) were recruited. The other eye of three patients was excluded from the study due to corneal scarring in 1 eye,

myopia in 1 eye, and hyperopic refraction $<+0.75$ diopters (D) treated in 1 eye. The mean time point at which the Artemis scan was performed was 10.6 ± 6.4 months (range: 2.6 to 24.3 months). The population mean age was 52.4 ± 8.9 years, median 52.0 years (range: 30.5 to 74.3 years). Mean attempted spherical equivalent refraction was $+3.84\pm 1.63$ D (range: $+0.75$ to $+7.13$ D), and mean attempted cylinder was 1.01 ± 1.04 D (range: 0.00 to 5.00 D). Mean postoperative maximum simulated keratometry was 48.10 ± 2.10 D (range: 43.20 to 52.60 D). Mean postoperative minimum simulated keratometry was 46.90 ± 2.00 D (range: 42.00 to 51.70 D).

B-scan

Figure 1 shows a non-geometrically corrected and a geometrically corrected horizontal cross-sectional B-scan image of a cornea 10 months after hyperopic LASIK for $+5.50 -2.00 \times 163$ obtained with the Artemis VHF digital ultrasound scanner. The epithelial thickness is visibly thinner in the center of the cornea and thicker paracentrally where the hyperopic ablation was deepest.

Epithelial Pachymetric Topography

The mean thinnest epithelial thickness for all eyes was 39.7 ± 5.6 μm (range: 26.9 to 52.7 μm) (95% confidence interval [39.0-40.4]). The thinnest epithelial point was displaced -0.19 ± 0.64 mm temporally and 0.93 ± 0.82 mm superiorly on average with reference to the corneal vertex.

The mean thickest epithelial thickness for all eyes was 89.3 ± 14.6 μm (range: 63.6 to 124.6 μm) (95% confidence interval [87.5-91.2]). The thickest epithelial point was displaced -2.49 ± 1.04 mm temporally and -0.73 ± 1.42 mm inferiorly on average with reference to the corneal vertex. The mean radial distance of the location of the thickest epithelium from the corneal vertex was 3.12 ± 0.25 mm (range: 2.3 to 3.6 mm).

Average, standard deviation, minimum, maximum, and range of epithelial thickness maps were studied (Fig 2). The epithelial thickness average map (see Fig 2) showed that the epithelium was thinner in a central, circular region approximately 4 mm in diameter with the thinnest epithelium in the superior half of this region. The central, thin epithelium was surrounded by an annulus of thicker epithelium, with the thickest epithelium temporally. The distance between the thickest epithelium at the peak of the annulus was 6.8 mm in the horizontal meridian and 6.7 mm in the vertical meridian.

The epithelial thickness standard deviation map (see Fig 2) showed there was more variation in epithelial thickness in the paracentral cornea with the least variation in epithelial thickness in an annulus with a radius of approximately 2 mm around the corneal vertex. The minimum epithelial thickness map (see Fig 2) demonstrated the thinnest epithelium within the study population to be within the central 4-mm diameter zone. The thinnest central epithelium was 28 μm , whereas the thinnest paracentral epithelium was 58 μm . The maximum epithelial thickness map (see Fig 2) showed that the thickest epithelium in the study population was found in a paracentral annulus surrounding the thin epithelium. The thickest epithelium was 116 μm located 3.1 mm temporal of the corneal vertex whereas the thickest epithelium within the central 4-mm diameter was only 56 μm . The range of epithelial thickness map

(see Fig 2) showed that the largest range in epithelial thickness in the study population was found in the paracentral annular region of epithelial thickening surrounding the thin epithelium. The smallest range of epithelial thickness was found within the central 4-mm zone.

Figure 3 shows the average preoperative, postoperative, and change in epithelial thickness profile for the subset of 10 eyes where preoperative data were available. The preoperative epithelial thickness profile demonstrated a similar pattern to that previously reported for a normal population³³; the epithelium was slightly thinner superiorly and temporally and slightly thicker inferiorly. The map of the average change in epithelial thickness demonstrated that the central epithelium was up to 8 μm thinner within the central 4-mm diameter zone and up to 24 μm thicker in an annular zone between the 4- and 8-mm diameters after LASIK. The fourth map in Figure 3 shows the P value at each point; the change in epithelial thickness was statistically significant ($P<.05$) in the center where the epithelium had become thinner and in the paracentral annulus where the epithelium had become thicker.

Figure 4 shows the cross-sectional, hemi-meridional epithelial thickness profile averaged for the population with the same data for a normal, untreated population also plotted for comparison.³³ Again, this highlights the thin epithelium centrally, with a minimum thickness of 46.9 μm , and the thick epithelium para-centrally, with a maximum thickness of 70.9 μm at a 3.4-mm radius from the corneal vertex. Within the central 1-mm radius, the annularly averaged epithelial thickness remained constant at an average of 46.9 μm . Between the 1- and 2-mm radius, the annularly averaged epithelial thickness started to gradually increase, reaching 50.9 μm at the 2-mm radius. Outside the 2-mm radius, the epithelial thickness increased significantly, reaching a maximum of 70.9 μm at a 3.4-mm radius before quickly becoming thinner again outside the 3.4-mm radius, down to 54.7 μm at the 3.8-mm radius.

Figure 5 shows the epithelial thickness profile for 15 eyes of the population selected at random using Microsoft Excel's random number function. Although all eyes exhibited the same epithelial annular pattern, the thickness values of the thinnest epithelium and thickest epithelium varied greatly in the population. For example, case 9 shows a minimum epithelial thickness of 49 μm and a maximum epithelial thickness of 79 μm . In contrast, case 12 shows a minimum epithelial thickness of 36 μm and a maximum epithelial thickness of 116 μm .

Figure 6 shows a scatterplot for the attempted spherical equivalent refraction for the thinnest and thickest epithelium. A statistically significant and strong correlation between the attempted spherical equivalent refraction and both the thinnest ($R^2=0.350$, $P<.001$) and the thickest epithelium ($R^2=0.765$, $P<.001$) was noted. This indicated that the minimum epithelial thickness was thinner and the maximum epithelial thickness was thicker in eyes after higher refractive ablations.

Figure 7 shows a scatterplot for the postoperative maximum simulated keratometry for the thinnest and thickest epithelium. A statistically significant correlation between the postoperative maximum simulated keratometry and both the thinnest ($R^2=0.210$, $P<.001$)

and thickest epithelium ($R^2=0.249$, $P<.001$) was noted. This indicated that the minimum epithelial thickness was thinner and the maximum epithelial thickness was thicker in eyes with steeper postoperative maximum simulated keratometry.

DISCUSSION

This is the first study to characterize the in vivo epithelial thickness profile over a 10-mm diameter area in a population of eyes after hyperopic LASIK. All eyes demonstrated an epithelial doughnut pattern characterized by a localized zone of thin epithelium surrounded by an annulus of thickened epithelium. We found an average epithelial thickness of 39.7 ± 5.6 μm at the central thinnest location and 89.3 ± 14.6 μm at the paracentral thickest location.

The average epithelium was up to 8 μm thinner centrally and up to 24 μm thicker at the 3.4-mm radius after LASIK in the subset of 10 eyes with preoperative data. The diameter of the annular zone of maximum epithelial thickening was 6.8 mm, which matches the programmed laser ablation optical zone diameter of 7 mm where the maximum ablation depth was at the 7-mm diameter. This demonstrates that the epithelium was compensating for the paracentral stromal tissue removal due to the hyperopic ablation.

As this was a retrospective case series, preoperative data were available for only 10 eyes, which may reduce the reliability of the results reported. However, there are a number of reasons why the lack of preoperative data should not affect the reliability or validity of the results. First, the epithelial thickness profile of the subset of 10 eyes with preoperative data was almost identical to that previously reported for a normal population of 110 eyes³³; the average central epithelial thickness was 52 μm in this subset of 10 eyes compared with 53 μm in the normal population of 110 eyes previously published.³³ Second, very little variation in epithelial thickness has been reported in untreated corneas, with a standard deviation of approximately 5 μm ^{6,33,36,37} and epithelial thickness ranging from 43 to 63 μm .³³ The range of epithelial thickness from 28 to 125 μm reported in the present study is well outside the range of epithelial thickness reported for untreated corneas. The magnitude of the difference between the epithelial thickness profile after hyperopic LASIK and that previously reported for normal eyes seems to provide compelling evidence that there has been an epithelial response to paracentral tissue ablation, which was confirmed by an identical result being found for the subset of 10 eyes with preoperative data.

Assuming that the preoperative epithelial thickness was ~ 53 μm for all eyes in the present study, the maximum postoperative epithelial thickness of 125 μm would translate to ~ 72 μm of epithelial thickening. This degree of epithelial thickening was significantly greater than the central epithelial thickening reported after myopic LASIK; we previously reported a maximum of 18 μm epithelial thickening after a -13.50 D myopic ablation.² This could be explained by the epithelial response according to the profile of tissue removed; hyperopic ablations induce a more abrupt change in curvature as the ablation must fit into half the cornea compared with myopic ablations where the change in curvature is more gradual across the diameter of the cornea. The epithelium appears to compensate more for a localized stromal irregularity. For example, Figure 8 shows a B-scan of a cornea where the epithelium has thickened by as much as 209 μm to compensate for stromal thinning caused

by a corneal ulcer (this scan was obtained with a prototype recti-linear VHF ultrasound scanner in 1996³). Given that the epithelium appears to be able to thicken more after a hyperopic ablation than a myopic ablation, the extra epithelial thickening in hyperopia may partly explain the greater degree of scatter in the refractive outcome that characterizes hyperopic LASIK³⁸⁻⁴⁰ compared with myopic LASIK.

Paracentral epithelial thickening has effectively reduced some of the shape change intended by stromal tissue ablation. Therefore, the epithelial thickness changes described in the present study would result in partial reversal of the hyperopic correction theoretically determined by the actual programmed stromal ablation. The central thinning of the epithelium also acts to flatten the cornea, which adds to the magnitude of the undercorrection. This could partly explain why early hyperopic ablation profiles resulted in large undercorrections (Eckhard Schroeder, PhD, Asclepion Meditec, oral communication, September 2001). It is plausible that epithelial thickness changes might also contribute to hyperopic regression, which has been described previously³⁸⁻⁴⁰; however, a longitudinal study of epithelial thickness changes correlated with refractive and topographic changes is required to confirm this.

The changes in epithelial thickness were correlated with the degree of hyperopic correction; the central epithelial thickness was thinner and the paracentral epithelial thickness was thicker for higher hyperopic corrections. This is similar to the epithelial changes seen after myopic ablations where there was more central epithelial thickening for higher myopic corrections,² which might partly explain why there is more regression seen in higher hyperopic corrections.³⁸⁻⁴⁰

The epithelial doughnut pattern observed in the current study population after hyperopic LASIK was in some ways similar to that seen in keratoconus,^{28,29} which is an expected result as a hyperopic ablation artificially creates a central and symmetric stromal cone. The minimum central epithelial thickness reported in the present study was 26.9 μm compared with 29.6 μm in advanced keratoconus, whereas the maximum paracentral epithelial thickness reported in the present study was 124.6 μm compared with 94.4 μm in advanced keratoconus.²⁸ Another similarity was that the central epithelium was thinner and paracentral epithelium was thicker for higher hyperopic corrections, just as the epithelium over the cone was thinner and epithelium around the cone was thicker for steeper keratoconic corneas.²⁸

It is currently assumed that hyperopic LASIK should be limited according to the postoperative curvature as too much steepening can result in epitheliopathy or apical syndrome; it is generally accepted that the postoperative curvature should not exceed 49.00 to 50.00 D.⁴¹ However, the results from the present study suggest that the central epithelial thickness may be a more useful indicator that further treatment may be attempted. The correlation of the postoperative maximum simulated keratometry and the thinnest epithelium suggests that whereas the thinnest epithelium is correlated with the postoperative curvature, the postoperative curvature alone can be misleading. In an example case from the present study, the maximum simulated keratometry of 50.80 D would most likely prevent the surgeon from treating further hyperopia; however, the central epithelial thickness of 41.7 μm

would suggest that the cornea could be steepened further without resulting in epithelial breakdown. On the other hand, another case from the present study demonstrates that the epithelial thickness can be thin (33.7 μm) although the cornea was still relatively flat postoperatively (46.40 D). The curvature limit would allow further hyperopic ablation, whereas the thin, central epithelium would indicate that further steepening might increase the risk of apical syndrome. Therefore, using epithelial thickness measurements, hyperopic retreatments might be performed without risk of apical syndrome while also allowing some patients to have retreatment who would otherwise have been rejected for further surgery due to high keratometry postoperatively.

The average epithelium in the present study was thinner in the superior half of the central 4-mm diameter zone, although the hyperopic ablations were symmetric and centered on the corneal vertex. Theoretically, it may have been expected that the thinnest epithelium would instead have been found at the corneal vertex. This result could theoretically be due to decentration of the ablation; however, the centration of the ablation profiles on the corneal vertex was confirmed by the symmetrical radial distance from the corneal vertex to the paracentral annulus of thick epithelium. Therefore, the superior shift of the thinnest epithelium must have a different explanation. We previously described the presence of thinner epithelium in the superior portion of the cornea in (untreated) normal corneas and found that the superior epithelium is on average 6- μm thinner than the inferior epithelium.³³ We postulated that this superior thinning is due to a chafing action of the upper lid—a mechanism that would still apply to the cases in this study.^{28,33}

A hyperopic ablation is symmetrical, so it might be expected that the epithelial changes would also be symmetrical. However, the average epithelium within the paracentral annulus of thick epithelium was 10- μm thicker temporally (81.2 μm) than nasally (71.4 μm). This finding was also demonstrated within the subset of 10 eyes with preoperative epithelial thickness data (see Fig 3) in that there was up to 24 μm of epithelial thickening temporally compared with 11 μm nasally. This asymmetry could plausibly induce some astigmatism. An analysis correlating the nasal/temporal epithelial asymmetry with the amount of induced cylinder found no correlation ($P=.118$). There are many other biomechanical factors that may influence the change in cylinder after hyperopic LASIK, and isolating the effect of the epithelium may prove difficult without more sophisticated analysis, including a multivariate regression analysis incorporating three-dimensional modeling, such as ray tracing, and is therefore outside the scope of this study. Given that the degree of epithelial thickening is correlated with the amount of tissue removed, this finding indicates that there was more ablation temporally than nasally. This is an interesting finding and we are currently investigating the potential causes.

This is the first published study to describe the characteristics of epithelial thickness profile changes after hyperopic LASIK. The epithelium was found to follow an epithelial doughnut pattern with thin epithelium within a central 4-mm diameter zone surrounded by an annulus of thick epithelium after hyperopic LASIK. The amount of epithelial thickening per diopter after hyperopic LASIK was greater than that reported after myopic LASIK and similar to that seen in advanced keratoconus. The reported change in the epithelial thickness profile

may partly explain hyperopic regression and could be used to improve the accuracy of hyperopic ablation, particularly with respect to induced cylinder.

Acknowledgments

Supported in part by NIH grant EB000238 and the Dyson Foundation, Millbrook, New York.

REFERENCES

1. Reinstein DZ, Archer T. Combined Artemis very high-frequency digital ultrasound-assisted transepithelial phototherapeutic keratectomy and wavefront-guided treatment following multiple corneal refractive procedures. *J Cataract Refract Surg.* 2006; 32:1870–1876. [PubMed: 17081871]
2. Reinstein DZ, Srivannaboon S, Gobbe M, Archer TJ, Silverman RH, Sutton H, Coleman DJ. Epithelial thickness profile changes induced by myopic LASIK as measured by Artemis very high-frequency digital ultrasound. *J Refract Surg.* 2009; 25:444–450. [PubMed: 19507797]
3. Reinstein DZ, Silverman RH, Trokel SL, Coleman DJ. Corneal pachymetric topography. *Ophthalmology.* 1994; 101:432–438. [PubMed: 8127563]
4. Reinstein DZ, Silverman RH, Sutton HF, Coleman DJ. Very high-frequency ultrasound corneal analysis identifies anatomic correlates of optical complications of lamellar refractive surgery: anatomic diagnosis in lamellar surgery. *Ophthalmology.* 1999; 106:474–482. [PubMed: 10080202]
5. Lohmann CP, Güell JL. Regression after LASIK for the treatment of myopia: the role of the corneal epithelium. *Semin Ophthalmol.* 1998; 13:79–82. [PubMed: 9758652]
6. Erie JC, Patel SV, McLaren JW, Ramirez M, Hodge DO, Maguire LJ, Bourne WM. Effect of myopic laser in situ keratomileusis on epithelial and stromal thickness: a confocal microscopy study. *Ophthalmology.* 2002; 109:1447–1452. [PubMed: 12153794]
7. Spadea L, Fasciani R, Necozone S, Balestrazzi E. Role of the corneal epithelium in refractive changes following laser in situ keratomileusis for high myopia. *J Refract Surg.* 2000; 16:133–139. [PubMed: 10766381]
8. Gauthier CA, Holden BA, Epstein D, Tengroth B, Fagerholm P, Hamberg-Nyström H. Role of epithelial hyperplasia in regression following photorefractive keratectomy. *Br J Ophthalmol.* 1996; 80:545–548. [PubMed: 8759267]
9. Lohmann CP, Reischl U, Marshall J. Regression and epithelial hyperplasia after myopic photorefractive keratectomy in a human cornea. *J Cataract Refract Surg.* 1999; 25:712–715. [PubMed: 10330651]
10. Reinstein DZ, Ameline B, Puech M, Montefiore G, Laroche L. VHF digital ultrasound three-dimensional scanning in the diagnosis of myopic regression after corneal refractive surgery. *J Refract Surg.* 2005; 21:480–484. [PubMed: 16209446]
11. Patel SV, Erie JC, McLaren JW, Bourne WM. Confocal microscopy changes in epithelial and stromal thickness up to 7 years after LASIK and photorefractive keratectomy for myopia. *J Refract Surg.* 2007; 23:385–392. [PubMed: 17455834]
12. Lohmann CP, Patmore A, Reischl U, Marshall J. The importance of the corneal epithelium in excimer-laser photorefractive keratectomy. *Ger J Ophthalmol.* 1996; 5:368–372. [PubMed: 9479520]
13. Lovisolo, CF.; Mularoni, A.; Calossi, A.; Stewart, CW. Complications of refractive keratotomy. In: Alio, J.; Azar, DT., editors. *Management of Complications in Refractive Surgery.* Springer-Verlag; Berlin, Germany: 2008. p. 197-224.
14. Reinstein DZ, Srivannaboon S, Holland SP. Epithelial and stromal changes induced by intacs examined by three-dimensional very high-frequency digital ultrasound. *J Refract Surg.* 2001; 17:310–318. [PubMed: 11383762]
15. Petroll WM, Goldberg D, Lindsey SS, Kelley PS, Cavanagh HD, Bowman RW, Parmar DN, Verity SM, McCulley JP. Confocal assessment of the corneal response to intracorneal lens insertion and laser in situ keratomileusis with flap creation using IntraLase. *J Cataract Refract Surg.* 2006; 32:1119–1128. [PubMed: 16857498]

16. Reinstein DZ, Gobbe M, Archer TJ, Couch D, Bloom B. Epithelial, stromal and corneal pachymetry changes during orthokeratology. *Optom Vis Sci.* 2009; 86:E1006–E1014. [PubMed: 19584769]
17. Swarbrick HA, Wong G, O’Leary DJ. Corneal response to orthokeratology. *Optom Vis Sci.* 1998; 75:791–799. [PubMed: 9848832]
18. Lu F, Simpson T, Sorbara L, Fonn D. Malleability of the ocular surface in response to mechanical stress induced by orthokeratology contact lenses. *Cornea.* 2008; 27:133–141. [PubMed: 18216565]
19. Sridharan R, Swarbrick H. Corneal response to short-term orthokeratology lens wear. *Optom Vis Sci.* 2003; 80:200–206. [PubMed: 12637831]
20. Haque S, Fonn D, Simpson T, Jones L. Epithelial thickness changes from the induction of myopia with CRTH RGP contact lenses. *Invest Ophthalmol Vis Sci.* 2008; 49:3345–3350. [PubMed: 18421075]
21. Reinstein, DZ.; Silverman, RH. Artemis VHF digital ultrasound technology. In: Wang, M., editor. *Corneal Topography in the Wavefront Era.* SLACK Incorporated; Thorofare, NJ: 2006. p. 207-226.
22. Reinstein, DZ.; Silverman, RH.; Archer, TJ. Very high frequency digital ultrasound: Artemis 2 scanning in corneal refractive surgery. In: Vinciguerra, P.; Camesasca, FI., editors. *Refractive Surface Ablation: PRK, LASEK, Epi-LASIK, Custom, PTK, and Retreatment.* SLACK Incorporated; Thorofare, NJ: 2006. p. 315-331.
23. Reinstein, DZ.; Archer, TJ. Evaluation of irregular astigmatism with Artemis very high-frequency digital ultrasound scanning. In: Wang, M., editor. *Irregular Astigmatism: Diagnosis and Treatment.* SLACK Incorporated; Thorofare, NJ: 2007. p. 29-42.
24. Reinstein DZ, Rothman RC, Couch DG, Archer TJ. Artemis very high-frequency digital ultrasound-guided repositioning of a free cap after laser in situ keratomileusis. *J Cataract Refract Surg.* 2006; 32:1877–1883. [PubMed: 17081872]
25. Scroggs MW, Proia AD. Histopathological variation in keratoconus. *Cornea.* 1992; 11:553–559. [PubMed: 1468218]
26. Haque S, Simpson T, Jones L. Corneal and epithelial thickness in keratoconus: a comparison of ultrasonic pachymetry, Orbscan II, and optical coherence tomography. *J Refract Surg.* 2006; 22:486–493. [PubMed: 16722488]
27. Aktekin M, Sargon MF, Cakar P, Celik HH, Firat E. Ultrastructure of the cornea epithelium in keratoconus. *Okajimas Folia Anat Jpn.* 1998; 75:45–53. [PubMed: 9715085]
28. Reinstein DZ, Gobbe M, Archer TJ, Silverman RH, Coleman DJ. Epithelial, stromal, and total corneal thickness in keratoconus: three-dimensional display with Artemis very high-frequency digital ultrasound. *J Refract Surg.* 2010; 26:259–271. [PubMed: 20415322]
29. Reinstein DZ, Archer TJ, Gobbe M. Corneal epithelial thickness profile in the diagnosis of keratoconus. *J Refract Surg.* 2009; 25:604–610. [PubMed: 19662917]
30. Reinstein DZ, Silverman RH, Coleman DJ. High-frequency ultrasound measurement of the thickness of the corneal epithelium. *Refract Corneal Surg.* 1993; 9:385–387. [PubMed: 8241045]
31. Reinstein DZ, Silverman RH, Rondeau MJ, Coleman DJ. Epithelial and corneal thickness measurements by high-frequency ultrasound digital signal processing. *Ophthalmology.* 1994; 101:140–146. [PubMed: 8302547]
32. Reinstein DZ, Silverman RH, Raevsky T, Simoni GJ, Lloyd HO, Najafi DJ, Rondeau MJ, Coleman DJ. Arc-scanning very high-frequency digital ultrasound for 3D pachymetric mapping of the corneal epithelium and stroma in laser in situ keratomileusis. *J Refract Surg.* 2000; 16:414–430. Erratum in *J Refract Surg.* 2001;7:4. [PubMed: 10939721]
33. Reinstein DZ, Archer TJ, Gobbe M, Silverman RH, Coleman DJ. Epithelial thickness in the normal cornea: three-dimensional display with Artemis very high-frequency digital ultrasound. *J Refract Surg.* 2008; 24:571–581. [PubMed: 18581782]
34. Reinstein DZ, Archer TJ, Gobbe M, Silverman RH, Coleman DJ. Stromal thickness in the normal cornea: three-dimensional display with Artemis very high-frequency digital ultrasound. *J Refract Surg.* 2009; 25:776–786. [PubMed: 19772263]

35. Reinstein DZ, Archer TJ, Gobbe M, Silverman RH, Coleman DJ. Repeatability of layered corneal pachymetry with the Artemis very high-frequency digital ultrasound arc-scanner [published online ahead of print November 16, 2009]. *J Refract Surg*. doi:10.3928/1081597X-20091105-01.
36. Wirbelauer C, Pham DT. Monitoring corneal structures with slitlamp-adapted optical coherence tomography in laser in situ keratomileusis. *J Cataract Refract Surg*. 2004; 30:1851–1860. [PubMed: 15342046]
37. Wang J, Thomas J, Cox I, Rollins A. Noncontact measurements of central corneal epithelial and flap thickness after laser in situ keratomileusis. *Invest Ophthalmol Vis Sci*. 2004; 45:1812–1816. [PubMed: 15161844]
38. Jaycock PD, O’Brart DP, Rajan MS, Marshall J. 5-year follow-up of LASIK for hyperopia. *Ophthalmology*. 2005; 112:191–199. [PubMed: 15691550]
39. Esquenazi S. Five-year follow-up of laser in situ keratomileusis for hyperopia using the Technolas Keracor 117C excimer laser. *J Refract Surg*. 2004; 20:356–363. [PubMed: 15307398]
40. Desai RU, Jain A, Manche EE. Long-term follow-up of hyperopic laser in situ keratomileusis correction using the Star S2 excimer laser. *J Cataract Refract Surg*. 2008; 34:232–237. [PubMed: 18242445]
41. Varley GA, Huang D, Rapuano CJ, Schallhorn S, Boxer Wachler BS, Sugar A, Ophthalmic Technology Assessment Committee Refractive Surgery Panel; American Academy of Ophthalmology. LASIK for hyperopia, hyperopic astigmatism, and mixed astigmatism: a report by the American Academy of Ophthalmology. *Ophthalmology*. 2004; 111:1604–1617. [PubMed: 15288995]

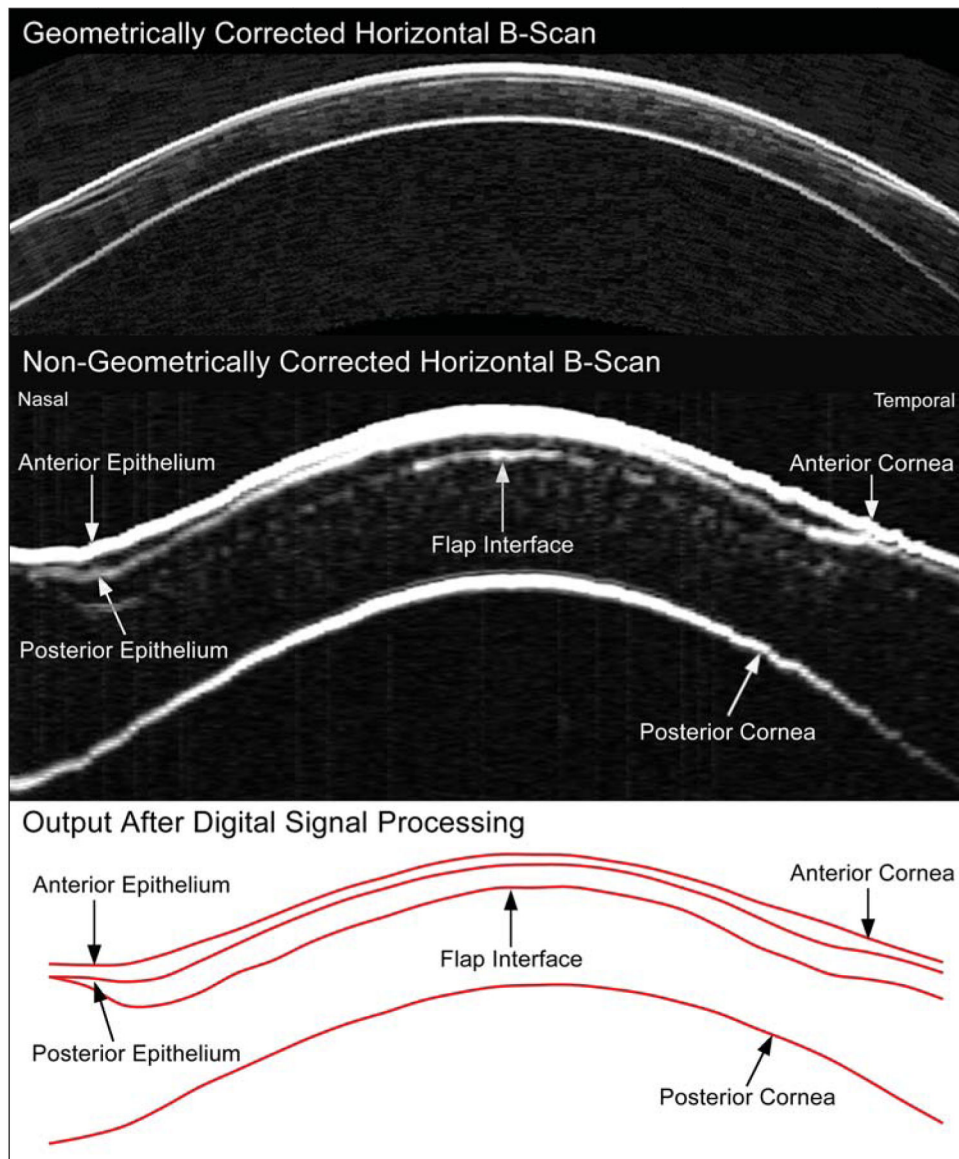


Figure 1.
Upper panel) Geometrically corrected horizontal B-scan image obtained using the Artemis very high-frequency (VHF) digital ultrasound arc-scanner. **Middle panel)** Non-geometrically corrected horizontal B-scan obtained using the Artemis VHF digital ultrasound arc-scanner. The image has been zoomed with different scales for the x and y axes; the width of the image corresponds to 10 mm whereas the height of the image corresponds to 1.2 mm. **Lower panel)** Digital signal processing is performed on the B-scan signal, and layer thickness measurements are obtained by a computer algorithm on the I-scan, resulting in the red line image of the interfaces.

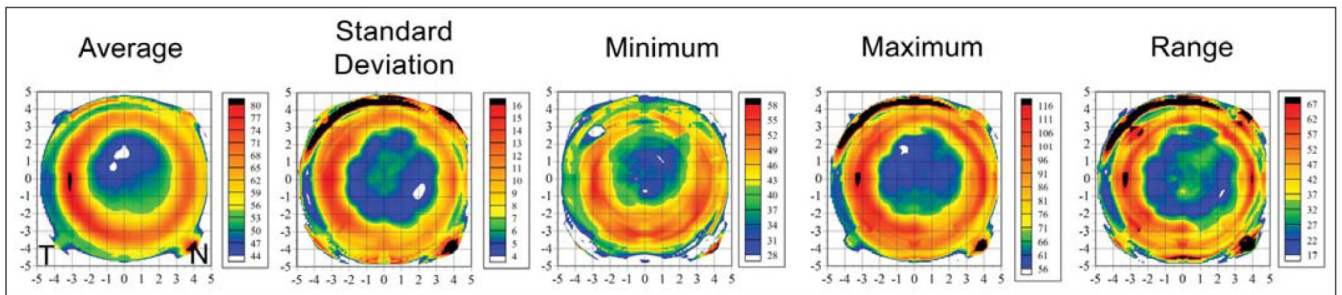


Figure 2.

Topographical map of the descriptive statistics of epithelial thickness centered on the corneal vertex for the population. All 65 eyes are included with left eyes mirrored (positive values represent the nasal cornea and negative values represent the temporal cornea). The color scale represents the epithelial thickness in microns. A Cartesian 1-mm grid is superimposed with the origin at the corneal vertex.

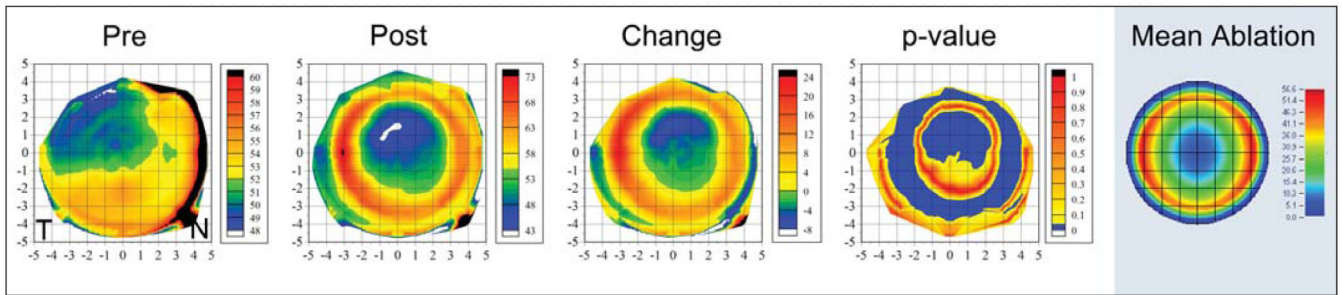


Figure 3.

Topographical map of the average preoperative, postoperative, and change in epithelial thickness profile for the subset of 10 eyes where preoperative data were available. A fourth map shows the point-by-point *P* value using Student paired *t* test. A fifth map shows the MEL 80 ablation profile for the mean hyperopic correction of this subset of 10 eyes: $+3.05 - 0.73 \times 180$. The epithelial thickness profiles were calculated with left eyes mirrored (positive values represent the nasal cornea and negative values represent the temporal cornea). The color scale for the pre- and postoperative maps represents the epithelial thickness in microns. The color scale for the change map represents the difference in epithelial thickness in microns; positive values indicate that the epithelium was thicker after LASIK and negative values indicate the epithelium was thinner after LASIK. The color scale for the *P* value map is set to show all points where there was a statistically significant change in blue ($P < .05$). The color scale for the ablation profile map represents the ablation depth in microns. A Cartesian 1-mm grid is superimposed with the origin at the corneal vertex.

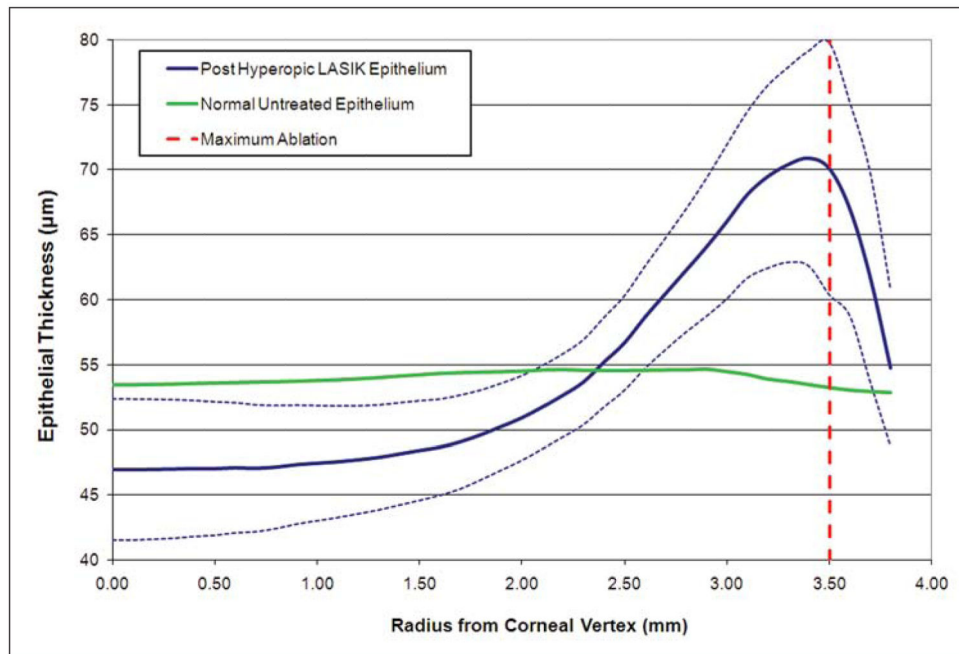


Figure 4.

Cross-sectional, hemi-meridional average epithelial thickness profile (μm) for all 65 eyes. The data points represent the average epithelial thickness of all data within an annulus of a given radius centered on the corneal vertex. The X axis is the radial distance (mm) from the corneal vertex. The thick blue line represents the average epithelial thickness profile and the dotted lines represent 1 standard deviation less than and 1 standard deviation greater than the average epithelial thickness. The thick green line represents the average epithelial thickness profile for a normal population.³³ The dotted red line represents the radius where the ablation was deepest; 3.50 mm for a 7-mm optical zone.

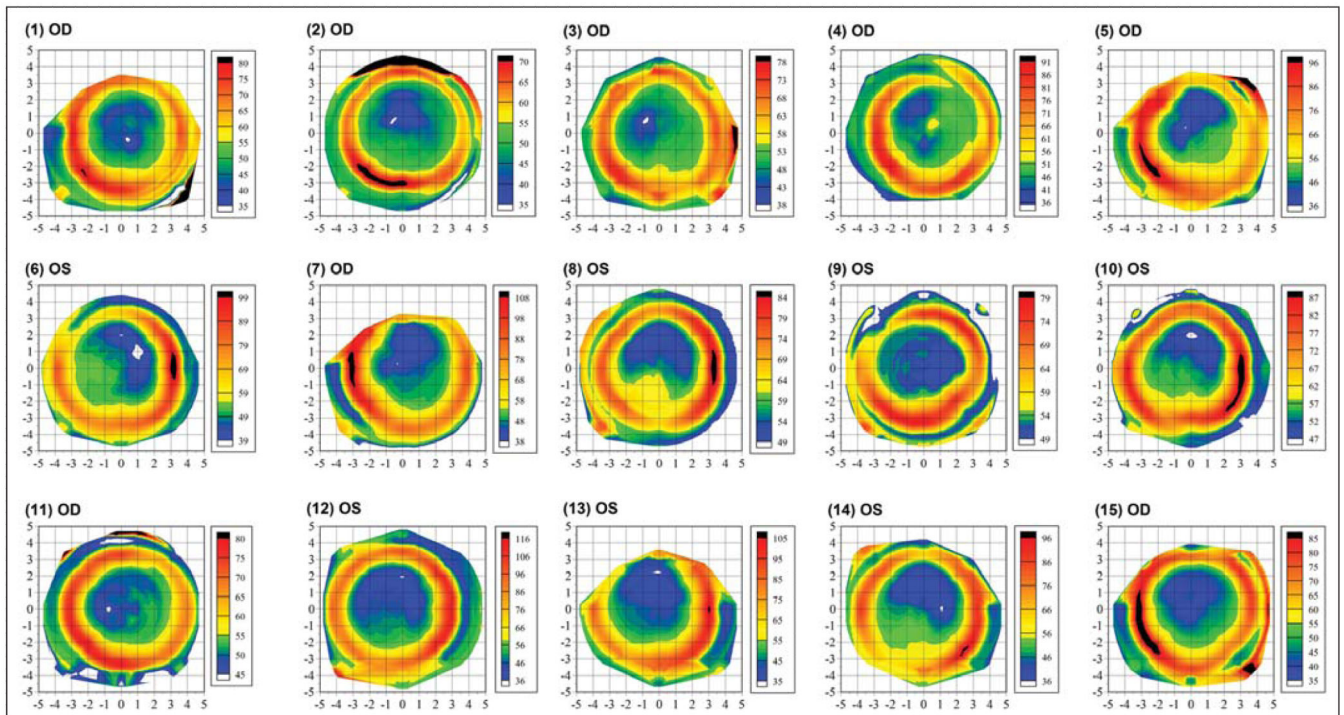


Figure 5. Epithelial thickness maps of 15 randomly selected eyes, each plotted with an individual color scale representing the epithelial thickness in microns. A Cartesian 1-mm grid is superimposed with the origin at the corneal vertex. OD = right eye, OS = left eye

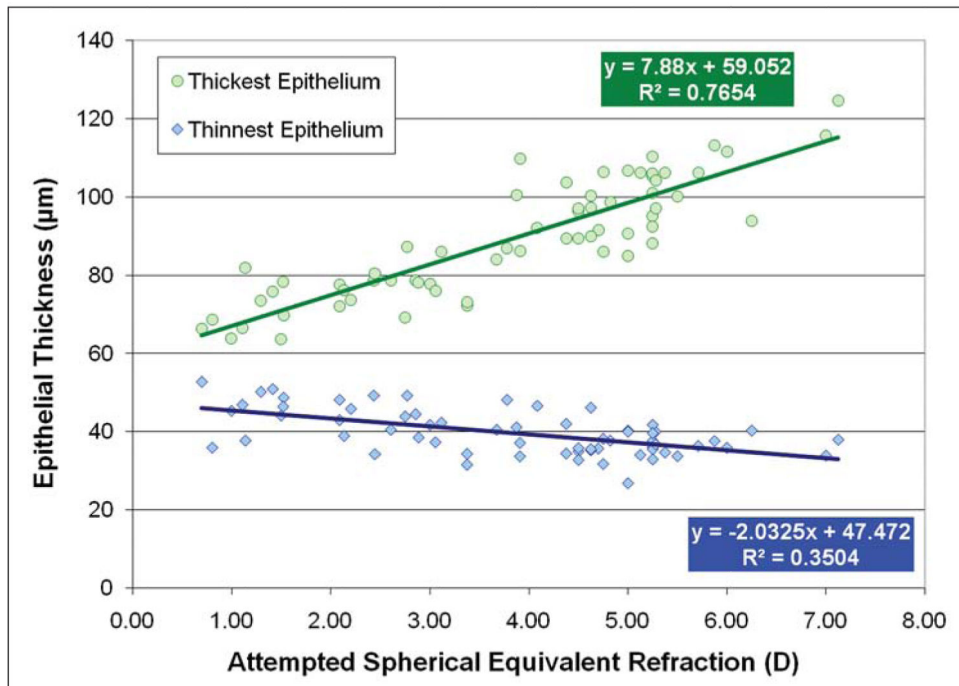


Figure 6. Correlation between the attempted spherical equivalent refraction (D) and the thinnest and thickest epithelium (μm). The linear regression equations and coefficients of determination (R^2) are indicated.

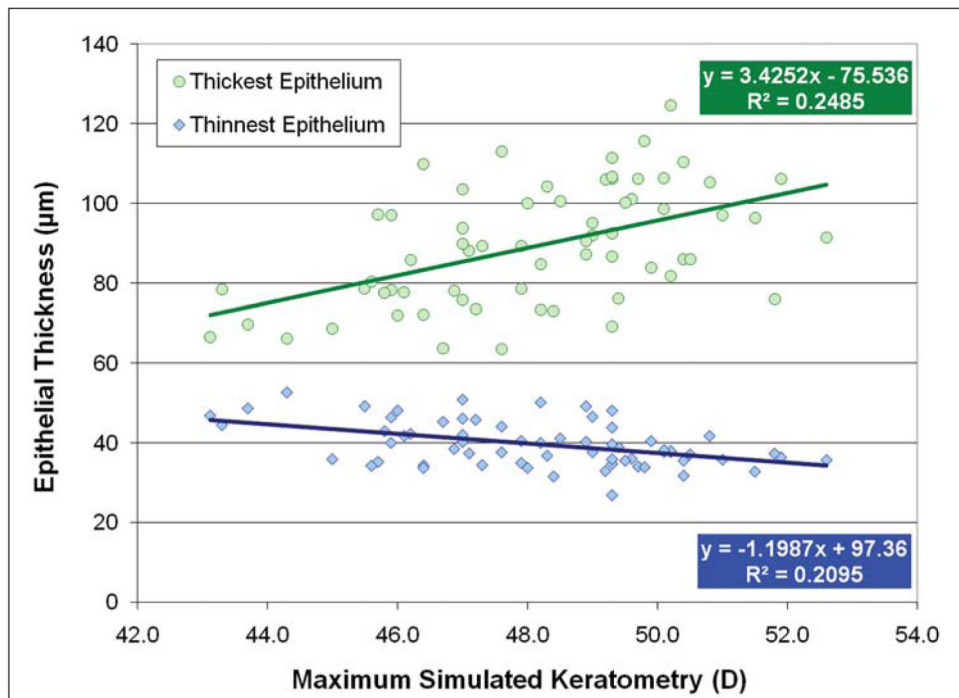


Figure 7. Correlation between the post-operative maximum simulated keratometry (D) and the thinnest and thickest epithelium (μm). The linear regression equations and coefficients of determination (R^2) are indicated.

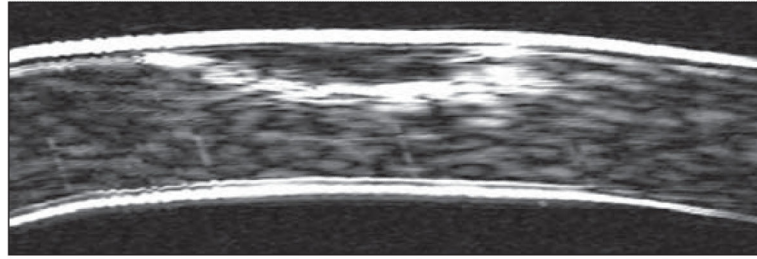


Figure 8.

Non-geometrically corrected very high-frequency digital ultrasound B-scan of the central 2 mm of a cornea after a corneal ulcer. The total corneal thickness is 536 μm and the epithelial thickness in the location of the corneal ulcer is 209 μm . The epithelial thickening over the region of the corneal ulcer has maintained a consistent curvature of the anterior surface of the cornea.